

High-brightness all semiconductor laser at 1.57 μm for space-borne lidar measurements of atmospheric carbon dioxide: device design and analysis of requirements

I. Esquivias , A. Consoli , M. Krakowski , M. Faugeron , G. Kochem , M. Traub , J. Barbero , P. Fiadino , X. Ai , J. Rarity , M. Quatrevalet , G. Ehret

ABSTRACT

The availability of suitable laser sources is one of the main challenges in future space missions for accurate measurement of atmospheric CO_2 . The main objective of the European project BRITESPACE is to demonstrate the feasibility of an all-semiconductor laser source to be used as a space-borne laser transmitter in an Integrated Path Differential Absorption (IPDA) lidar system. We present here the proposed transmitter and system architectures, the initial device design and the results of the simulations performed in order to estimate the source requirements in terms of power, beam quality, and spectral properties to achieve the required measurement accuracy. The laser transmitter is based on two InGaAsP/InP monolithic Master Oscillator Power Amplifiers (MOPAs), providing the ON and OFF wavelengths close to the selected absorption line around 1.57 μm . Each MOPA consists of a frequency stabilized Distributed Feedback (DFB) master oscillator, a modulator section, and a tapered semiconductor amplifier optimized to maximize the optical output power. The design of the space-compliant laser module includes the beam forming optics and the thermoelectric coolers. The proposed system replaces the conventional pulsed source with a modulated continuous wave source using the Random Modulation-Continuous Wave (RM-CW) approach, allowing the designed semiconductor MOPA to be applicable in such applications. The system requirements for obtaining a CO_2 retrieval accuracy of 1 ppmv and a spatial resolution of less than 10 meters have been defined. Envelope estimated of the returns indicate that the average power needed is of a few watts and that the main noise source is the ambient noise.

Keywords: Earth observation from space, differential absorption lidar, semiconductor lasers, random modulation continuous wave lidar, integrated master oscillator power amplifiers, laser frequency locking.

1. INTRODUCTION

Atmospheric distribution of carbon dioxide plays a fundamental role in understanding of global warming and climate change. Observation of CO_2 distribution on planetary scale is then relevant for accurate modeling and prediction of Earth climate dynamics. At present, the concentrations of CO_2 are mainly measured in-situ at a number of surface stations that are unevenly distributed over the planet. Air-borne and space-borne missions have the potential to provide a denser and better distributed set of observations to complement this network.

In the framework of European Project BRITESPACE [1], we propose an all-semiconductor laser source for an Integrated Path Differential Absorption (IPDA) [2] lidar for column-averaged measurements of atmospheric CO_2 in future space mission.

IPDA lidar can provide column-averaged CO_2 measurement by sounding the atmosphere at two wavelengths which are relevant for the gas under study: one wavelength is set near the center of a CO_2 absorption line (on-line channel, λ_{ON}) and the other is set close to but off the same line (off-line channel, λ_{OFF}). Both wavelengths are close enough to exhibit almost identical aerosol attenuations, but will exhibit different CO_2 absorptions. The attenuation from CO_2 molecules can

be calculated by the power ratio of the back-scattered signals at the end of the optical path and can be converted into a column-averaged mixing ratio thanks to the knowledge of the path length from the round-trip time delay.

Typical laser sources currently used in IPDA lidars are solid state lasers working in pulsed regime, emitting ns pulses with high energy at low to medium repetition rate (typical values are 10-50 ns, ~10-50 mJ, 50-200 Hz) [3, 4]. Although these laser systems have demonstrated the high average power, high laser beam quality and frequency stability required by the application, it is at the expense of a bulky system with low wall plug efficiency, which is a main concern for space-borne applications. Numata et al. [5] have investigated on hybrid Master Oscillator Power Amplifiers (MOPAs) combining a Distributed Feedback (DFB) semiconductor laser as seed laser and Erbium Doped Fiber Amplifiers working in pulsed conditions in the context of NASA mission ASCENDS. However, the use of active optical fibers in space applications requires specific attention to the radiation shielding, orbit and the duration of the flight, since it is known that fiber amplifier materials have low radiation hardness [6].

All-semiconductor laser sources are very interesting candidates for space-borne atmospheric sensing applications, due to their compactness, high efficiency, reliability, and radiation hardness. However, they cannot produce the high energy pulses needed in standard pulsed IPDA lidar. In order to circumvent this intrinsic limitation, Random Modulation CW (RM-CW) [7] lidar technique is proposed for use with semiconductor lasers in a IPDA system, as the required output power is suitable for use with semiconductor lasers. In RM-CW lidar, a Pseudo Random Binary Sequence (PRBS) is transmitted, and the received signal correlated with the original PRBS code, giving range resolved response with non-ambiguous range as determined by the number of PRBS bits.

This manuscript is organized as follows: in Section 2 the design of the laser transmitter and of the entire system is presented and detailed description is given of laser chip, laser module and FSU. In Section 3, we present the numerical modeling of the complete IPDA lidar and simulations results are presented for estimating the system performances. Finally, in Section 4, the main conclusions are summarized.

2. LASER TRANSMITTER AND SYSTEM DESIGN

The design of the complete IPDA lidar system is shown in Fig. 1. It consists of the laser transmitter, the optics for beam transmission and reception and the control electronics. Specifically, the output beam from the transmitter is split in two branches: one is sent to the beam expander and then to the atmosphere and the other is used as reference in the comparison with the received signal, for the calculation of CO₂ concentration. The reflected light from Earth ground is collected by a reflective telescope with a Field of View (FOV) matching the laser beam divergence and alignment issues are addressed by using a short wave infrared (SWIR) camera.

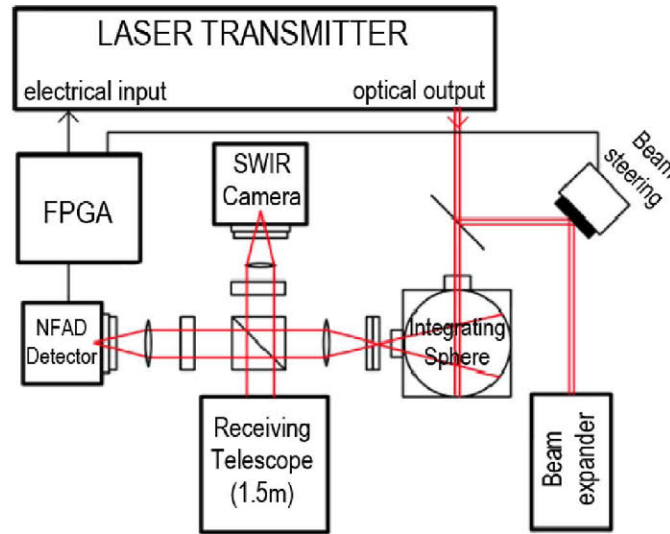


Fig. 1. Block scheme of the complete IPDA lidar.

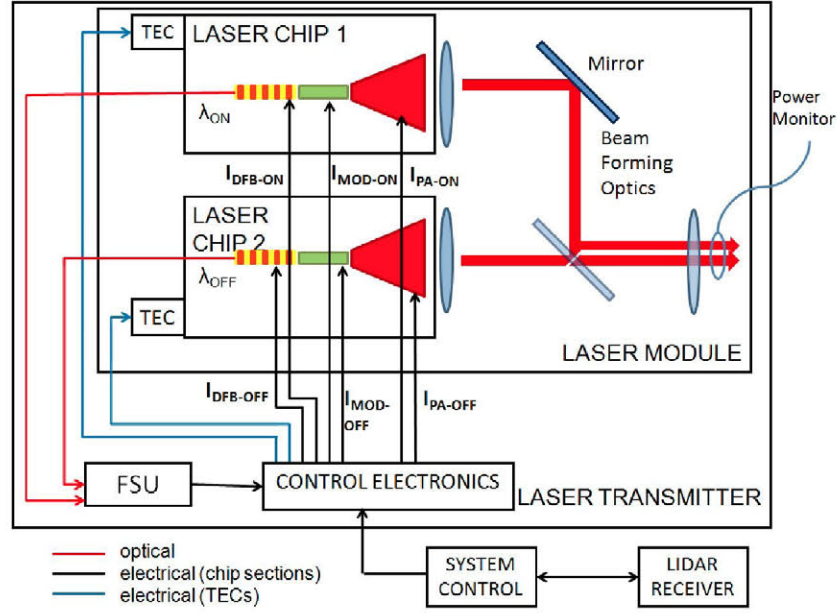


Fig. 2. Block scheme of the laser transmitter.

A very high sensitivity detector based on InGaAs negative feedback avalanche diodes (NFAD) is proposed for single photon counting of the received signal [8]. The modulation sequence and the decorrelation process required by the RM-CW technique are implemented with a Field Programmable Gate Array (FPGA).

The laser transmitter architecture is shown in Fig. 2. It consists of a space compatible Laser Module, the control electronics and the Frequency Stabilization Unit (FSU). Two Laser Chips, one for each sounding frequency (λ_{ON} , λ_{OFF}) required for CO₂ detection in IPDA systems, are housed in the Laser Module, together with the beam forming optics and two power monitoring photodiodes. The back facet output of the Laser Chips are sent to the FSU through standard SMF for frequency stabilization. In the following, Laser Chips, Laser Module and FSU are described in detail.

2.1 Laser Chip

A set of two InGaAsP/InP monolithic MOPAs is proposed as the main building block of the Laser Transmitter. Each MOPA is a three section device, consisting of a frequency stabilized Distributed Feedback (DFB) master oscillator, a modulator section, and a tapered amplifier. The use of this original structure aims to fulfill the performances required by the IPDA system in terms of high power, frequency stability and good beam quality. In this sense, the DFB section is accurately frequency stabilized in an external opto-electrical feedback loop through the FSU (see further in the text). The modulator section is introduced for implementation of the RM-CW technique in the proposed IPDA system. Finally, the geometry of the tapered amplifier is optimized in order to provide high brightness output beam with sufficient power and beam quality.

More in detail, three different geometries are proposed for the Laser Chip implementation, which are based on: *straight*, *tilted* and *bended* designs, shown in Fig. 3. The straight geometry consists of a standard structure in which the oscillator, modulator and amplifier sections are in-line with the propagation axis and perpendicular to the output facet (i.e. the tilt angle is 0°). The tilted and bended geometries are proposed in order to minimize undesired optical feedback from the amplifier section to the DFB oscillator. In fact, standard straight monolithically integrated MOPAs are typically characterized by non linear behavior due to compound cavity effects from residual reflectivity at the amplifier output facet [9, 10].

We expect that the tilted and bended geometries will allow linear operation of the device, at different operating points, as required by the RM-CW in the modulator section. Standard straight MOPA geometry will also be fabricated and used as a reference for comparison with the other two geometries.

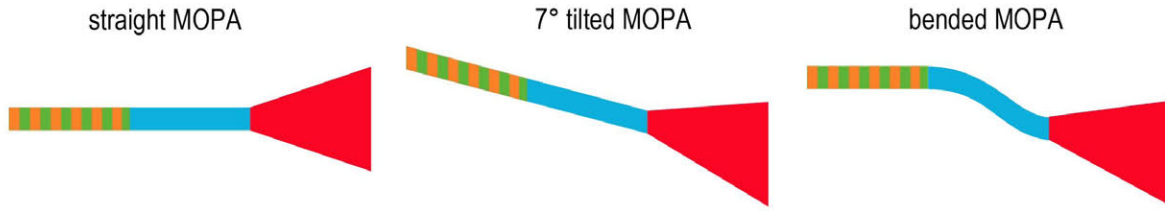


Fig 3. Straight, tilted and bended geometry designs for Laser Chip fabrication.

The design of the epitaxial structure of the devices is optimized in order to decrease the internal losses, which are relevant on InP based devices, and reduce the output beam divergence in the vertical direction. It is based on a dilute slab asymmetrical cladding approach [11] and multiple Quantum Well (QW) active region. Preliminary results on fabricated broad area lasers with the mentioned epitaxial design have shown promising results in terms of low internal losses (7.3 cm^{-1}), low threshold current density ($<480 \text{ Acm}^{-2}$), low vertical divergence (32°) and high internal quantum efficiency (93%).

2.2 Laser Module

For each Laser Chip, a sub-module has been designed in order to provide electrical access, temperature control and beam forming optics for each MOPA. Figure 4 shows the design of a sub-module and the complete module, in Figs. 4 a) and b), respectively. The radiation emitted by the tapered amplifier is astigmatic, i.e. it has different source points (and different angles of divergence) in the fast axis (vertical direction) and slow axis (horizontal direction). Due to this characteristic an optical system for the collimation of a tapered amplifier must consist of two lenses [12]. We propose the use of a first aspheric lens and a second cylindrical lens. The first lens is for collimation of the fast axis and intermediate focusing of the slow axis. The second cylindrical lens collimate the slow axis and does not affect the fast axis beam. Considering also the tilted and bended geometries for Laser Chips, the emitter is tilted in slow axis in order to achieve perpendicular propagation.

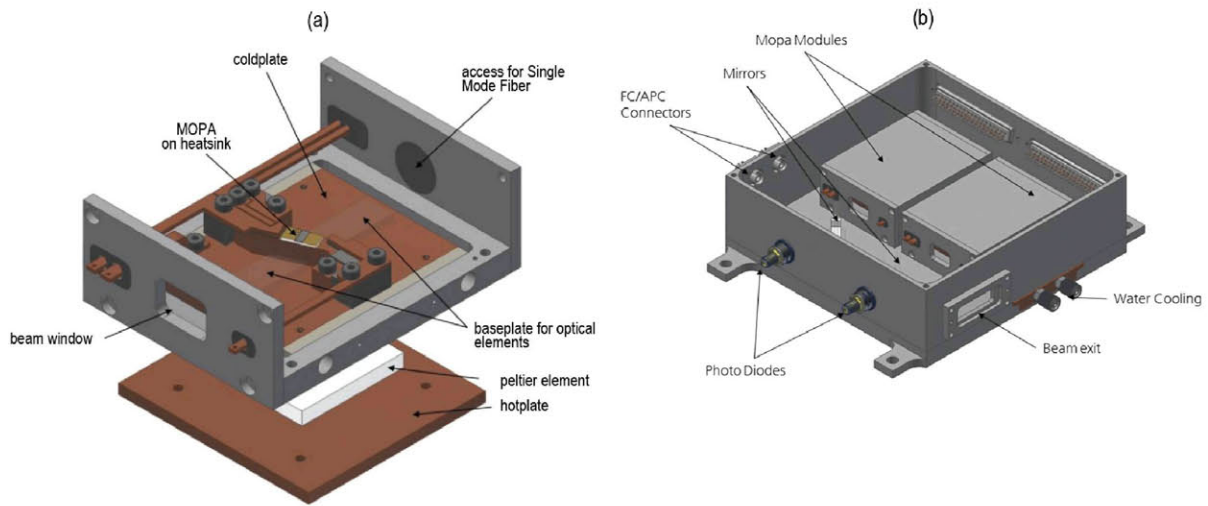


Fig. 4. Laser sub-module (a) and module (b).

The radiation emitted from the back facet of the DFB is expected to be diffraction limited, and therefore can be coupled into a lensed Single Mode Fiber (SMF) aligned to the DFB back facet.

Two mirrors, one for each sub-module, are used for combining the output beams before exiting the Laser Module. Partially reflective mirrors will be used in order to allow power monitoring for each MOPA with two photodiodes placed

right after the combining mirrors. Laser beam from the two Laser Chips are placed close each other at the Laser Module output, for minimizing footprint errors in IPDA detection.

2.3 Frequency Stabilization Unit

IPDA lidar systems require high frequency stabilization for accurate estimation of gas molecule concentration, in order to have precise measurement of the detected power ratio at the selected absorption line [2]. We propose the use of two opto-electrical feedback loops for the stabilization of the on- and off- channels emitted by the MOPAs. A simple scheme, showing the selected design for the FSU, is presented in Fig. 5.

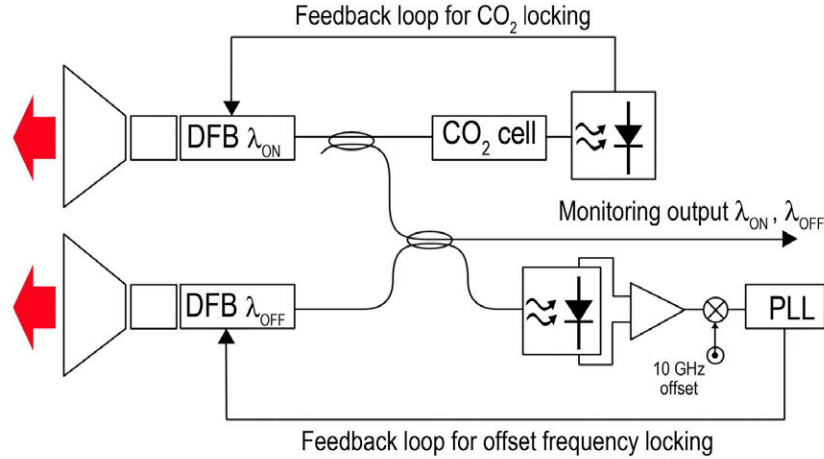


Fig. 5. Block scheme of the proposed Frequency Stabilization Unit.

Light emitted from the back facet of the DFB section of the on- channel MOPA will be collected through a lensed SMF fiber and sent to a 50:50 fiber coupler. One of the output port of the coupler is sent to the on-channel locking feedback loop and the other is combined with the light emitted from the back facet of the off- channel MOPA with a second 50:50 fiber coupler. The on-channel MOPA will be locked to the selected CO₂ absorption line using a multi pass CO₂ reference cell and a custom feedback loop based on a commercially available (LaseLock, TEM Messtechnik GmbH) laser frequency locking equipment. A second feedback loop will be used to stabilize the beat note of the on- and off- channel signal at a fixed 10 GHz offset. The on- and off- channels frequency locking loops are schematically depicted in Fig. 4, where only the main components are shown: the CO₂ reference cell, the 10 GHz signal generator and the Phase Locked Loop (PLL), all based on the LaseLock equipment.

3. NUMERICAL SIMULATIONS

3.1 CW-RM IPDA lidar model

In this section, we derive the model for a RM-CW lidar from a simple analysis of a conventional pulsed system. In a IPDA pulsed system, the transmitted pulse power, $P^T(t)$, can be described for each channel, by $P^T(t) = P^K(t) \cdot \delta(t) * G_p(t)$, where $P^K(t)$ is the pulse peak power, $\delta(t)$ is the Dirac function, $G_p(t)$ is the shape of the transmitted laser pulse and $*$ is the convolution operator.

The received pulse power, $P^R(t)$, can be written for each channel as $P^R(t) = P^K(t) \cdot \delta(t) * G_p(t) * G_a(t)$, where $G_a(t)$ is the atmosphere response function, given by $G_a(t) = \eta_0 \cdot S_p \cdot T_{on,off} \cdot A_r \cdot R^{-2} \cdot \delta(t - \tau)$, with η_0 the optical efficiency of the receiver, S_p the surface parameter (equal to reflectivity divided by π), A_r the area of the telescope, R the orbit altitude, T_{on} and T_{off} , the on- line and off- line transmittance and τ the time delay from ground reflection.

In a CW-RM IPDA lidar, the transmitted signal is described with a random impulse train $III_T(t)$, given by $III_T(t) = \sum a_k \delta(t - kT_C)$ where a_k is the PRBS, T_C is the period of the impulse train and k a positive integer. The received optical signal is then given, for each channel, by $P^R(t) = [P^K(t) \cdot III(t) * G_p(t)] * G_a(t)$.

Differently from a pulsed IPDA lidar, where the on- channel and the off- channel are transmitted and received sequentially, in a RM-CW IPDA lidar, both wavelength are transmitted and detected at the same time. Discrimination of each channel is obtained by shifting in time one code with respect to the other and by separate decoding at the receiver. The total received power is then given by:

$$P_{TOT}^R(t) = P_{on}^K \cdot III_T(t) * G_p(t) + P_{off}^K \cdot III_T(t - \Delta T) * G_p(t) \quad (1)$$

where P_{on}^K and P_{off}^K are the peak powers of the on- and off- channel, respectively, and ΔT is the time shift applied.

Finally, the background contribution is removed by correlating the received signal with $III_T(t)$ and its negated $\overline{III_T}(t)$ and subtracting:

$$P^R = P_{TOT}^R * III_T(-t) - P_{TOT}^R * \overline{III_T}(-t) \quad (2)$$

3.2 Estimation of Signal to Noise Ratio

In the following sub-section, the noise performance of the system in space-borne scenarios is investigated. It has been identified that the major noise contributor of the proposed system will be ambient noise and detector dark noise. Similar to previous derivations, the Signal to Noise Ratio (SNR) will be first described for the pulsed approach. For the pulsed scheme, the received pulse energy $E_{on,off}^R$ is concentrated within a single range gate (main reflection from the ground). Signal shot noise is proportional to the square-root of the number of photoelectrons integrated in this range gate, $N_{on,off} = \xi_e E_{on,off}^R$, in which ξ_e denotes the photon energy to photoelectron number conversion coefficient (see Tab. 1). Ambient light and detector noise equivalent photoelectron numbers are represented by N_{amb} and N_{det} per range gate.

Following the shot-noise statistics, the SNR of the pulsed method can be approximated by:

$$SNR_{on,off}^{pul} = \frac{N_{on,off}}{\sqrt{N_{on,off} + N_{amb} + N_{det}}} \quad (3)$$

To compare the SNR of the CW-RM system with respect to the pulsed system, it will be assumed that both systems have the same average transmission power, which yields the same total received signal photoelectron numbers $N_{on,off}$ after correlation. A CW-RM system under such conditions will receive less photoelectrons per range gate, as energy is spread over m (number of '1's in the PRBS) range gates, while the received photoelectrons counts per range gate are reduced by a factor of m . The number of photoelectrons for ambient light N_{amb} and noise equivalent photoelectrons N_{det} per gate remain the same as the pulsed system. In the CW-RM system, the cross-correlation effectively accumulates the photoelectrons numbers for m range gates. Hence, a high level of noise photoelectrons $m \cdot N_{amb}$ and $m \cdot N_{det}$ per integration time is to be expected. Therefore, the SNR of the RM-CW can be calculated as:

$$SNR_{on,off}^{RM-CW} = \frac{N_{on}}{\sqrt{2(N_{off,on} + N_{on,off} + m \cdot N_{amb} + m \cdot N_{det})}} \quad (4)$$

Note that in Eq. (4), the $\sqrt{2}$ term in the noise term is caused by the subtraction of two correlations described in Eq. (2). Both N_{on} and N_{off} are in the noise term at the denominator, because both on- and off- channels are transmitted and received simultaneously during each retrieval, as commented previously.

According to Eq. (4), for the CW-RM system to approach to the measurement precision of the pulsed system with similar average transmitting power, the ambient light level and detector noise need to be reduced.

The retrieval accuracy of the CO₂ mixing ratio is obtained as:

$$\sigma_{XCO_2} = \frac{XCO_2}{2 \cdot DAO D} \sqrt{(SNR_{on}^{RM-CW})^2 + (SNR_{off}^{RM-CW})^2} \quad (5)$$

Simulation results are shown in Tab. 1. We obtain a CO₂ retrieval precision for the proposed system of 1.5 ppm. Although this value is at the boundary of future IPDA mission specifications, it's worth noting that we considered the

worst case scenario, as the surface reflectivity used in calculations refers to that of the ocean (which has the lowest surface albedo). For measurements taken across vegetation, the CO₂ retrieval precision is improved.

Table 1. Envelope SNR estimation for a space-borne RM-CW IPDA lidar.

<p><i>Transmitter</i></p> <p>On-line average power: $P_{on}^{avg} = 2 \text{ W}$</p> <p>Off-line average power: $P_{off}^{avg} = 2 \text{ W}$</p> <p>Chip (bit) time: $T_C = 40 \text{ ns}$</p> <p>Integration time: $T_{int} = 7 \text{ s}$</p> <p>On-line wavelength: $\lambda_{ON} = 1572.02 \text{ nm}$</p> <p>Off-line wavelength: $\lambda_{OFF} = 1572.11 \text{ nm}$</p> <p><i>Receiver</i></p> <p>Type: Cassegrain telescope</p> <p>Area: $A_r = 1.77 \text{ m}^2$</p> <p>Bandpass filter FWHM: $\Delta\lambda = 800 \text{ pm}$</p> <p>Optical efficiency: $\eta_0 = 80 \%$</p> <p>FOV (full): $\theta_{FOV} = 50 \mu\text{r}$</p> <p><i>Detector</i></p> <p>Type: Multiple channel Geiger mode NFADs</p> <p>Detection efficiency: $\eta_e = 30\%$</p> <p>Detector dark count: $N_{dc} = 500 \text{ Kcps}$</p> <p><i>Misc.</i></p> <p>Orbit type: 6-h sun synchronous</p> <p>Solar Zenith angle: $\theta_{zen} = 75^\circ$</p> <p>Nadir radiance (ocean-veg): $L_r = 1.7 \text{ mWm}^{-2} \text{ nm}^{-1} \text{ sr}^{-1}$</p> <p>Orbit altitude: $R = 450 \text{ km}$</p> <p>Velocity: $v = 7 \text{ km/s}$</p> <p>Surface albedo (ocean-veg): $\alpha_s = 0.03 \text{ sr}^{-1}$</p> <p>On/off-line transmittance: $T_{on} = 0.3 \text{ } T_{off} = 0.78$</p> <p>DAOD: DAOD = 0.48</p> <p>CO2 mixing ratio: XCO2 = 400 ppm</p>	<p><i>Calculated values</i></p> <p>Photoelectron coeff: $\xi_e = \eta_e \lambda_{on} / hc = 2.37 \text{e}18$</p> <p>On-line photoelectrons accumulated :</p> $N_{on} = P_{on}^{avg} \cdot T_{int} \cdot \eta_0 \cdot \frac{\alpha_s}{\pi} \cdot T_{on} \cdot \frac{A_r}{R^2} \cdot \xi_e = 3.2M$ <p>Off-line photoelectrons accumulated:</p> $N_{off} = P_{off}^{avg} \cdot T_{int} \cdot \eta_0 \cdot \frac{\alpha_s}{\pi} \cdot T_{off} \cdot \frac{A_r}{R^2} \cdot \xi_e = 8.2M$ <p>Ambient photoelectrons accumulated :</p> $mN_{amb} = mT_C \cdot \eta_0 \cdot \Delta\lambda \cdot L_r \cdot \left(\frac{\theta_{FOV} R}{2} \right)^2 \cdot \frac{A_r}{R^2} \cdot \xi_e = 42.5 M$ <p>Detector equivalent photoelectrons:</p> $mN_{det} = mT_C \cdot N_{dc} = 1.75M$ <p>On-line SNR :</p> $SNR_{on}^{RM-CW} = \frac{N_{on}}{\sqrt{2(N_{off} + N_{on} + mN_{amb} + mN_{det})}} = 298$ <p>Off-line SNR:</p> $SNR_{off}^{RM-CW} = \frac{N_{off}}{\sqrt{2(N_{off} + N_{on} + mN_{amb} + mN_{det})}} = 778$ <p>XCO2 accuracy:</p> $\sigma_{XCO2} = \frac{XCO2}{2 \cdot DAOD} \sqrt{(SNR_{on}^{RM-CW})^{-2} + (SNR_{off}^{RM-CW})^{-2}} = 1.50 \text{ ppm}$
---	---

4. SUMMARY

In this paper, we propose an all semiconductor laser source at 1.57 μm for space-borne lidar measurements of atmospheric carbon dioxide concentration. The complete design of the proposed CW-RM IPDA lidar has been presented and described in detail. Two MOPAs, emitting at the sounding frequency of the on- and off- IPDA channels, are proposed as the transmitter optical sources with the required high brightness.

The complete transmitter architecture has been proposed and the laser chips, laser module and frequency stabilization unit are presented in detail. The CW-RM approach has been modeled and an estimation of the expected SNR for the entire system is presented. Promising results indicate that a CO₂ retrieval precision of 1.5 ppm could be achieved with an average output power of 2 W for each channel.

ACKNOWLEDGEMENT

This work was supported by the European Commission through the project BRITESPACE under grant agreement no. 313200.

REFERENCES

- [1] <http://www.britespace.eu/>
- [2] G. Ehret, C. Kiemle, M. Wirth, A. Amediek, A. fix And S. Houweling., "Space-borne remote sensing of CO₂, CH₄, and N₂O by integrated path differential absorption lidar: a sensitivity analysis" *Applied Physics B*, 90 (3-4), 593-608 (2008).
- [3] Browell, E., S. Ismail, and W. Grant, "Differential absorption lidar (DIAL) measurements from air and space" *Applied Physics B*, 67(4), 399-410 (1998).
- [4] Fix, A., et al., "Water vapor differential absorption lidar measurements using a diode-pumped all-solid-state laser at 935 nm" *Applied Physics B*, 102(4), 905-915 (2011).
- [5] Numata, K., et al., "Frequency stabilization of distributed-feedback laser diodes at 1572 nm for lidar measurements of atmospheric carbon dioxide" *Applied Optics*, 50(7), 1047-1056 (2011).
- [6] Fox, B.P., et al., "Gamma-radiation-induced photodarkening in unpumped optical fibers doped with rare-earth constituents" *IEEE Transactions on Nuclear Science*, 57(3), 1618-1625 (2010).
- [7] Ai, X., et al., "High-resolution random-modulation cw lidar" *Applied Optics*, 50(22), 4478-4488 (2011).
- [8] Ai, X., et al "Pseudo-random Single Photon Counting for Space-borne Atmospheric Sensing Applications". *IEEE Aerospace Conference 2014*. Big Sky, Montana, USA.
- [9] M. Spreemann, M. Lichtner, M. Radziunas, U. Bandelow, and H. Wenzel, "Measurement and simulation of distributed feedback tapered master-oscillator power-amplifiers" *IEEE Journal of Quantum Electronics* 45(6), 609-616 (2009).
- [10] S. Bauer, O. Brox, J. Kreissl, B. Sartorius, M. Radziunas, J. Sieber, H. J. Wünsche, and F. Henneberger, "Nonlinear dynamics of semiconductor lasers with active optical feedback," *Phys. Rev. E* 69, 016206 (2004).
- [11] M. Faugeron, M. Tran, O. Parillaud, M. Chtioui, Y. Robert, E. Vinet, A. Enard, J. Jacquet, and F. Van Dijk, "High-Power Tunable Dilute Mode DFB Laser With Low RIN and Narrow Linewidth", *IEEE Photonics Technology Letters*, 25(1), 7-10 (2013).
- [12] Gerd Kochem ; Mark Haverkamp ; Konstantin Boucke, "Frequency stabilized high brightness tapered amplifier and laser modules " *Proc. SPIE 6997* (2008)
- [13] Joel F. Campbell, Bing Lin, and Amin R. Nehrir "Advanced sine wave modulation of continuous wave laser system for atmospheric CO₂ differential absorption measurements" *Applied Optics*, 53(5), 816-829 (2014).